On the Influence of Hull Girder Flexibility on the Wave

Seng, Sopheak; Andersen, Ingrid Marie Vincent; Jensen, Jørgen Juncher

Published in:
Proceedings of the 6th International Conference on Hydroelasticity in Marine Technology

Publication date:
2012

Document Version
Publisher's PDF, also known as Version of record

Proceedings of the sixth International Conference on Hydroelasticity in Marine Technology
Tokyo, JAPAN
19-21 September 2012

HYDROELASTICITY IN MARINE TECHNOLOGY

Edited by

Ken TAKAGI
The University of Tokyo, JAPAN
and
Yoshitaka OGAWA
National Maritime Research Institute, JAPAN

First published 2012

The University of Tokyo
5-1-5, Kashiwanoha, Kashiwa, Chiba

ISBN 978-4-9906321-0-6

Printed in Japan by TOSEI PRINTING Co., Ltd.

ON THE INFLUENCE OF HULL GIRDER FLEXIBILITY ON THE WAVE INDUCED BENDING MOMENTS

Sopheak Seng, Ingrid Marie Vincent Andersen, and Jørgen Juncher Jensen
Section of Fluid Mechanics, Coastal and Maritime Engineering
Technical University of Denmark, 2800 Kgs. Lyngby, Denmark

ABSTRACT

Numerical predictions and model test results of the wave induced bending moments in a 9,400 TEU post-Panamax container vessel are presented for two regular wave scenarios. Different numerical procedures have been applied: a linear and non-linear time-domain strip theory and a direct calculation (CFD) solving the Navier-Stokes equations with the free surface captured by a volume-of-fluid (VOF) method. In all procedures the flexibility of the hull girder is modelled as a non-uniform Timoshenko beam. It is observed that the non-linear models agree well with the model tests and as there is no occurrence of severe slamming in the cases considered, the inexpensive non-linear strip theory is as accurate as the direct CFD calculation method. In a comparison with the results using the rigid body assumption, the increase in the vertical bending moment (VBM) amidships due to the flexibility of the hull girder is found to be approximately 7% (peak-to-peak amplitude) in general. The non-linear responses, however, contain over-harmonic frequencies which may coincide with the natural frequency of the two-node vertical bending mode inducing resonance. In that case the hull girder flexibility causes the responses to increase as much as 22% (peak-to-peak amplitude) in one of the present cases.

KEYWORDS

hydroelasticity; fluid-structure interaction; CFD; VOF; non-linear strip theory; Timoshenko beam

1. INTRODUCTION

With the increasing size of container vessels concern has been expressed about the importance of the hull girder flexibility on structural responses in waves. Specifically, a number of full scale and model tests have shown that a significant increase in the wave induced bending moment can occur in realistic seaways and operational conditions[1,2,3]. One of the important issues that affect a large vessel is that the encounter frequency is more likely to be within the range of the natural frequencies of the hull girder vibration causing whipping and springing responses to occur more frequently. Due to the higher flexibility of the larger ship and the risk of resonance excitation of the structural modes a calculation method based on the rigid body assumption is no longer necessarily accurate enough. Hence, there is a need to include the flexibility of the hull girder in both experimental and numerical studies.

There are several published experimental measurements of large flexible vessels; see e.g. Ref.[1,2,3]. The model test results presented in Zhu et al.[2] suggest that vertical bending moment (VBM) in regular head sea waves may contain high-frequency components with amplitude approximately proportional to the wave height squared. Even though there were too few

measurement data to make this relationship conclusive, the results clearly demonstrate a strong nonlinear dependency with regard to the wave height. In Miyake et al.[3] the hydroelastic response of a 12,000 TEU container ship was investigated experimentally using a scale model. Springing was observed in regular head sea waves where the non-linear hydrodynamic forces induce a resonance with the 2nd over-harmonic. The induced hydroelastic responses due to springing produced a large vertical bending moment in the hull girder. The ratio between the wave length and the length of the ship was as small as 0.265 resulting in almost no pitch motion. Most importantly, the experimental results show a large variation, revealing the high sensitivity of the responses at resonance.

To approach the hydroelastic hull girder problem numerically a fluid solver needs to be coupled to a structural solver. The most advanced, but also structurally most complicated model is the 3D FEM model. Alternatively, a Timoshenko beam model can be applied; see e.g. Ref[4-7]. Xia et al.[5] based the calculations on a time-domain non-linear strip theory. Only vertical bending is included in the beam model. Recent attempt has been to couple a CFD based fluid solver with the Timoshenko beam model cf. el Moctar et al.[8]. The fluid solver solves the Reynolds-Averaged Navier Stokes (RANS) equations with the free surface captured by a volume-of-fluid (VOF) technique. The hydrodynamic damping and the relevant flow features are implicitly included in the hydrodynamic forces. As a result the springing and the whipping responses are also implicitly included. The major issue seems to be the requirement of the computational power. As mentioned in el Moctar et al.[8] the CFD mesh needs to be fine enough to minimize numerical induced damping and diffusion. Applying the fine mesh in a combination with a small time step size a modern high-performance computer (HPC) cluster is usually required. Other issues are related to the amplitude of the predicted hydroelastic vibration and to obtaining grid independent results. Nevertheless, the predicted responses compared reasonably well with the measurements.

A similar free surface CFD method (NS/VOF using OpenFOAM) is applied in this paper to address hydroelastic effects due to the flexible hull girder and its contribution to the wave induced vertical bending moment. A comparison is made with another method based on a linear and non-linear strip theory[5]. The same structural model is applied in both procedures i.e. the hull girder is modelled as a non-uniform Timoshenko beam with realistic parameters, including stiffness and mass distribution, taken from the model test configuration, but scaled to the real vessel. The analyses are presented as a case study of a 9,400 TEU post-Panamax container vessel sailing in head sea at 15 knots. The main parameters of the ship are shown in Table 1. Two incident regular long-crested waves are considered, both with wave amplitude of 4 m. The first wave, Case #004 in the model test program of EU FP7 project TULCS (Tools for Ultra Large Container Ships), has a period of 14.9 s producing a wave length to ship length ratio of 1. The second wave (Case #014) has a wave period of 11.66 s, corresponding to a wave length approximately 0.65 of the length between perpendiculars; see also Table 2. The steepness of the target waves are approximately 0.023 and 0.037 for Case #004 and Case #014, respectively. The model tests were done by CEHIPAR, an independent public research center in Spain and the results of the measurements will be compared with the numerical results. The model tests were done on a scale model (1:80) built with an aluminium backbone, designed to reflect the structural properties of the flexible hull girder of a specific real post-Panamax vessel. Only head sea is considered.

TABLE 1
MAIN PARAMETERS OF THE POST-PANAMAX SHIP

-	Full scale	Model (1:80)
Overall Length, Loa, [m]	349	4.363
Length btw. Pp., Lpp, [m]	333.43	4.168
Breadth, [m]	42.8	0.535
Draught, [m]	13.1	0.164
Mass, [ton]	$1256 \cdot 10^6$	0.2393

TABLE 2
THE TARGET WAVE PARAMETERS AND THE EXPERIMENTS BY CEHIPAR

Regular wave	Target		Exp. CEHIPAR		Rel. Err.	
	H [m]	T [s]	H (min, max) [m]	T (min, max) [s]	H	T
Case #004	8	14.90	8.32 (7.88, 8.86)	14.92 (14.89, 14.99)	4.0 %	0.13 %
Case #014	8	11.66	8.66 (7.80, 9.19)	11.70 (11.56, 11.85)	8.25 %	0.34 %

2. NUMERICAL METHOD

An in-house non-linear time-domain strip-theory sea-keeping code (Shipstar[5]) which is capable of predicting non-linear wave loads and ship responses is applied. The non-linear hydrostatic restoring forces and the non-linear Froude-Krylov forces are estimated exactly over the instantaneous wetted surface. Furthermore, the non-linear memory effect due to the free surface are included using a rational fractional approximation of the sectional added mass m and damping N in terms of the encounter frequency cf. Tick[9]:

$$i\omega m - N = \frac{\sum_{j=0}^{J} A_j (-i\omega)^{j+1}}{\sum_{j=0}^{J} B_j (-i\omega)^{j}} \tag{1}$$

where $A_j(x)$ and $B_j(x)$ are functions of the sectional geometry only. These coefficients are determined by a least square fit to the results from a singularity distribution mapping procedure[10]. Usually only a few terms ($J = 3$ or 4) are needed in order to achieve accurate results. Thereby it is straightforward to formulate a non-linear procedure taking into account the variation of added mass and damping with the instantaneous sectional submergence[5]. Finally, Shipstar also includes a standard momentum slamming term. More recently Shipstar has been applied in Ref.[11] to do an extreme value analysis for large vessels taking into account the flexibility of the hull girder.

The free surface NS/VOF simulations performed in the present study are carried out using the open source CFD tool box OpenFOAM®. The software package provides a multiphase fluid solver known as “interDyMFoam” which is a finite volume Navier Stokes solver for two incompressible and immiscible fluids where the interface is captured using a volume of fluid (VOF) approach. Included in the fluid solver there is an optional mesh motion with an arbitrary Lagrangian-Eulerian (ALE) momentum formulation. The surface tension force has very limited effect on the flow and is therefore neglected. The transport equation which describes the evolution of the volume fraction function i.e. the free surface, is modified to prevent numerical smearing of the interface by including a compression term defined to be active only at the interface; see Berberović et al.[12].

The simulation will be carried out for the full scale ship moving head sea at 15 knots. The corresponding Froude number is 0.135 and the Reynolds number is in the order of $O(10^9)$. Physically, the hull experiences a resistance force induced mainly by the incident wave, the ship generated wave and viscous shear stresses. The viscous related loads have a significant contribution to the resistance force implying a need for a turbulence model when dealing with resistance calculations. In the present simulation, however, only the vertical wave loads are assumed to be importance for the structural deformation of the hull girder. Therefore no turbulence model has been applied in the simulation.

The ALE formulation allows body motion to be defined in terms of dynamic motion of the body boundaries. The grid points on the moving body are moved according to the required motion of the body. The internal grid points, however, can be moved more freely. The only constraint applied to the internal grid points is that the finite volume mesh remains valid and the quality of each cell remains sufficiently good. A mesh morphing technique utilizing the solution of a

Laplacian of the grid-point displacement has been applied to determine the movement of internal grid points[13]. The distribution of the diffusivity coefficient in the Laplacian equation is set according to the inverse quadratic distance to the moving boundaries yielding a small relative displacement for points close to the moving body which helps to preserve the quality of the near boundary cells. The same mesh morphing technique has been applied successfully in previous papers[14,15].

To simulate a flexible ship moving in head sea the OpenFOAM CFD toolbox has been extended with a structural solver where the flexibility of the hull girder is modelled as a non-uniform Timoshenko beam. Only the planar vertical deformation is considered. The formulation is the same as in the non-linear strip theory code Shipstar. The equations of motions are written cf.[16]:

$$\frac{\partial}{\partial x}\left[EI\left(1+\mu\frac{\partial}{\partial t}\right)\frac{\partial \phi}{\partial x}\right]+kGA\left(1+\varepsilon\frac{\partial}{\partial t}\right)\left(\frac{\partial v}{\partial x}-\phi\right)-mr^2\frac{\partial^2\phi}{\partial t^2}=0 \tag{2a}$$

$$\frac{\partial}{\partial x}\left[kGA\left(1+\varepsilon\frac{\partial}{\partial t}\right)\left(\frac{\partial v}{\partial x}-\phi\right)\right]-m\frac{\partial^2 v}{\partial t^2}=-f(x,t) \tag{2b}$$

where *m, r, EI, kGA* are the mass, radius of gyration, and structural stiffness properties of the hull defined as non-uniform beam. The symbol v denotes the vertical deflection and ϕ denotes the angular deformation. It is assumed that the damping coefficients μ and ε are equal and independent of the longitudinal position x. The forcing term *f(x,t)* is the total force acting on the hull i.e. the external force which are mainly the fluid force, the gravitational force and the body forces related to whether the equations are solved on the ship-fixed or the Newtonian frame of reference.

A means to solve Eq. (2) is to use a modal superposition method[16] where dry mode shapes of the free-free Timoshenko beam are used to describe the structural deformation. The deflection *v(x,t)* and the angular deformation $\phi(x,t)$ are written in terms of preselected dry mode shapes as

$$v(x,t)=\sum_{j}^{N}u_j(x)w_j(t) \tag{3a}$$

$$\phi(x,t)=\sum_{j}^{N}\varphi_j(x)w_j(t) \tag{3b}$$

The eigenfunctions u_j and φ_j are dry mode shapes corresponded to planar vertical deformation of the free-free Timoshenko beam which can be determined using e.g. Stodola's method[17]. The dry mode shapes are orthogonal in the sense that

$$\int_{x_{\min}}^{x_{\max}}(mr^2\varphi_i\varphi_j+mu_iu_j)dx=\begin{cases}0 & for \quad \omega_i\neq\omega_j\\ A_j & for \quad \omega_i=\omega_j\end{cases} \tag{4}$$

where ω_j is the natural frequency corresponding to the mode shape j. Assuming $\mu=\varepsilon$ and applying the orthogonality condition Eq. (4), the equation for the time dependent modal coefficient $w_j(t)$ become

$$\ddot{w}_j(t)+\mu\omega_j^2\dot{w}_j(t)+\omega_j^2w_j(t)=\frac{1}{A_j}\int_{x_{\min}}^{x_{\max}}u_j(x)f(x,t)dx \tag{5}$$

It shall be emphasized that Eqs. (5) are coupled because the hydroelastic coupling implies that the external force depends on the deflection of the ship. The external force *f(x,t)* is a priori unknown and needs to be determined from the fluid solver. Iterations are performed to assure an implicit strong coupling between the external force and the deflection of the hull girder. The equations (5) are integrated individually using a second order predictor-corrector Adam-Moulton scheme:

$$\theta = \theta_0 + \frac{\Delta t}{2}\left[(2+\tau)\dot{\theta}_0 - \tau\dot{\theta}_{00}\right] \tag{6a}$$

$$\theta^k = \theta_0 + \frac{\Delta t}{16\tau}\left[(8\tau+1)\dot{\theta}^{k+1} + (7\tau-1)\dot{\theta}_0 + \tau\dot{\theta}_{00}\right] \tag{6b}$$

where θ represents the modal coefficient w_j in any mode. The time steps are $\Delta t = t - t_0$ and $\tau = \Delta t/(t_0 - t_{00})$ where the subscript 0 and 00 denote the previous values; one and two steps back, respectively. At the initial time step where previous solutions are not available the explicit Euler integration scheme is applied.

The coupling between the fluid solver and the motion solver is critical and a strong implicit coupling is important to maximize the stability of the numerical solution. The coupling scheme applied in the present simulation is the same as the partitioned strong coupling scheme presented in previous paper[15]. The fluid solver provides the total force *f(x,t)* to the motion solver where the rigid body motion and planar vertical deflection are solved for. The fluid mesh as well as the corresponding fluid solution is updated and the iteration continues until convergence. The feedback from the motion solver is mainly the new location of the boundary points presenting the moving hull and the structural deformations. In a Newtonian frame of reference these points are updated as

$$\mathbf{x} = \mathbf{x}_{cog} + \mathbf{R}\mathbf{R}_0^T(\mathbf{x}_{flex} - \mathbf{x}_{0,cog}) \tag{7}$$

where $\mathbf{x}_{cog}$ is the present location vector of the center of mass; the subscript 0 denotes the initial values and $\mathbf{R}$ is the rotation matrix of the rigid body motion. The structural deflection and the present position of points on the deformed ship i.e. $\mathbf{x}_{flex}$ are calculated in the ship-fixed coordinate system. Thus, at any time instant the vector $\mathbf{x}_{flex}$ is computed using the initial position $\mathbf{x}_0 = (x, y, z)$ as

$$\mathbf{x}_{flex} = \mathbf{v}(x) + \mathbf{Q}^T(x)(\mathbf{x}_0 - \mathbf{x}_{0,flex}(x)) \tag{8}$$

where $\mathbf{v}(x)$ and $\mathbf{x}_{0,flex}(x)$ are respectively the present vertical deformation and the initial deflection given at the longitudinal position x. The rotation matrix $\mathbf{Q}$ is a function of x and is computed according to the local total angular deformation i.e. the rotation of the cross-section due to bending and shear consistent with the Timoshenko beam theory. Between the structural solver and the flow solver information is passing back and forth creating a two-way strong hydroelastic coupling scheme.

In order to determine the importance of hydroelasticity for the present calculations, an option in the coupling scheme is to neglect the elastic deformation of the hull girder in the flow solver. The hydrodynamic and hydrostatic load distributions are determined from a rigid body simulation. Thereafter, these load distributions are used to estimate the elastic effect of the hull girder. This scheme creates a one-way coupling between the Timoshenko beam solver and the fluid solver since the deformation of the ship is calculated purely as a post-processing task. This shall not be confused with the so-called weak coupling approach where the deformation of the hull girder is transferred to the fluid solver once in every time step. The fluid solver does not get any information about the deformation of the hull girder in the one-way coupling approach. The

feasibility of applying this option will be discussed by making a comparison with the results of the more complicated and time-consuming two-way coupling scheme and the experimental measurements.

3. NUMERICAL SETUP

The simulation is done in full scale. The length between perpendiculars (L_{pp}) for the post-Panamax ship is 333.43 m and the breadth is 42.8 m. The size of the domain (wave tank) is chosen to be 1575x350x300 m in length, width and water depth, respectively. The ship is moving in head sea and only half of the ship is included in the simulation, due to symmetry. The inlet is located about 1.5 L_{pp} in front of the ship and the wake region behind the ship is approximately 2 L_{pp}. A numerical beach with a length of L_{pp} is located at the outlet and the size of whole domain is considered sufficiently large to avoid wave reflection from the boundaries.

A sketch of the computational domain and the grid configuration is shown in Fig. 1. The grid is fitted to the hull using split-hexahedral and polyhedral cells. The cells are clustered near the hull, the free surface and the wave propagation zone in front of the ship. Within the wave propagation zone the average horizontal grid spacing is approximately 1 m which is a sufficient resolution for Case #004 and Case #014, where the wave length is approximately 349 m and 217 m, respectively. Numerical tests reveal that the wave is dissipating very slightly as it propagates through the domain. The rate of the dissipation is less than 0.1% per wave length. The final mesh has approximately 4.2 millions cells.

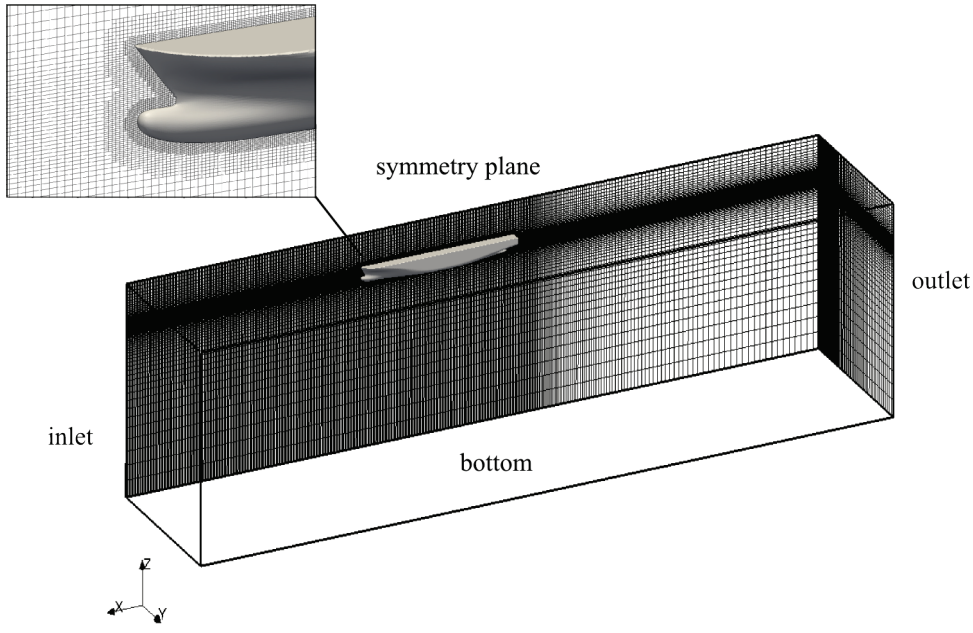

Figure 1: A sketch of the grid configuration (4.2 millions cells)

At the inlet boundary the kinematics of the wave i.e. the position of the free surface and velocity profile are prescribed according to the solution of a high-order stream function wave theory[18]. At the outlet boundary a relaxation zone is introduced to minimize wave reflection. The technique to relax the out-going wave follows the method applied in previous papers[14,15]. The constant forward speed is accounted for using a moving frame of reference. The boundary conditions for the primitive variables including the volume fraction which defines the free surface elevation are updated and defined with respect to the moving frame of reference.

It is well known that a three dimensional free surface CFD simulation with VOF method is very expensive in terms of computational resources. The requirement of the processing power is even larger when the VOF method is applied to simulate waves and the related transient flow behaviour. Furthermore, before waves can be activated at the inlet boundary, the flow needs to be in a quasi-steady state corresponding to the ship moving forward at a constant speed in calm water. The huge demand on the processing power is of today a major barrier preventing the free surface CFD simulation method to be widely used in practical engineering applications. The performance seen in the present simulations is on average 4 hours for every simulated second using a high performance Intel® Xeon® X5550 cluster with 64 cores. One of the most time consuming parts is the inner iteration of the implicit strong coupling fluid-structure interaction scheme done at each time step. While the size of the time step is dynamically adjusted, the average step size is about 0.005 s. The results of the full scale simulations are compared against scale model experiments converted to full scale using the Froude's scaling law. Due to the huge demands on the processing power, the results for the fine mesh (4.2 million cells) are used in the comparison without a grid convergence study.

The Timoshenko beam solver requires the one dimensional line load $f(x,t)$ from the fluid solution. At each time step, fluid pressures in three-dimension are converted to one-dimensional line loads using cross-section interpolations[15]. The line loads are evaluated at 128 longitudinal positions distributed appropriately along the hull. The static structural and load properties such as mass per unit length $m(x)$, $EI(x)$, $kGA(x)$ and $r^2(x)$ are shown in Fig. 2. Dry natural frequencies reported by CEHIPAR are 0.682 Hz for the 2-node mode and 1.588 Hz for the 3-node mode with the corresponding damping ratio 1.6% and 1.5%. The damping ratios are estimated from random vibration tests and it has been reported that the 3-node mode response is low yielding a large uncertainty in the estimate. In CFD simulations the damping ratio has been set to 1% considering the fact that the structural damping ratio may take a different value and is difficult to predict accurately at full scale. Moreover, the contribution from the structural damping is usually small compared to the effect of the hydrodynamic damping. From Fig. 2 it is seen that the estimated 2-node vertical vibration agrees well with the experimental measurements. For the higher modes the agreement is less encouraging. Measured responses in waves, however, show that the hull is vibrated mostly in 2-node mode and the contribution of the higher modes is small.

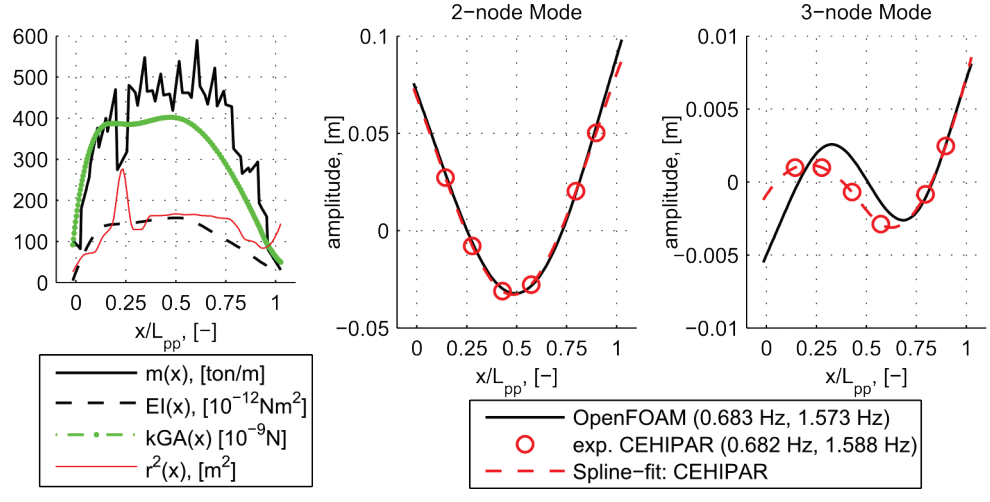

Figure 2: Structural properties and the estimated dry modes in a comparison with experimental measurements by CEHIPAR (2-node and 3-node planar vertical bending modes)

4. RESULTS AND DISCUSSION

Using the Froude's scaling law the results of the experiments are converted to full scale and compared with the numerical predictions. In the comparisons the time axes are synchronized using the estimated wave profile at the amidships section. With the applied loading condition the ship is in hogging condition in calm water. According to the rigid body simulation the VBM amidships at the quasi-steady state becomes 5488 MNm. When accounting for the flexibility of the hull girder, the VBM decreases to 5187 MNm. The numerical wave generator is activated at the inlet when a steady state condition is obtained. In strip theory (Shipstar) there is no need to simulate the wave field around the ship. The incident wave can be applied almost instantaneously everywhere. A start-up time of 5 s, however, has been applied in Shipstar to obtain a smooth introduction of the wave field. The start-up duration is longer with the free surface CFD simulation (OpenFOAM) since waves need to propagate transiently from the inlet to the ship. Once the incident wave reaches the ship it will take additionally a few more wave periods for the ship to reach a quasi-steady heave and pitch motion. The numerical results for Case #004 shows that the required time to reach a steady heave and pitch motion is about 5 wave periods (see Fig. 3) whereas Case #014 requires about 10 wave periods. This time depends strongly on the forward speed (Froude number) and the particular wave configuration. A rough estimate of the required start-up time can be obtained using a simple linear single-degree-of-freedom damped mass-spring system with damping ratio ξ and natural frequency ω_n. Assuming that the excitation force is purely harmonic the time to reduce the amplitude to 5% of the initial value is

$$\Delta t = -\frac{\ln(5\%)}{\xi\omega_n} \tag{9}$$

As an example; for $\xi = 1.5\%$ and $\omega_n = 0.56$ rad/s the required time is 356 s. From the CFD calculation point-of-view this is a long time implying that it is crucial to start up the motion and excitation smoothly. There is, however, the possibility that the motion will never become stationary if there is strong non-linearity in the system. Even small non-linearities may lead to chaotic response behaviour.

It should also be stressed that there are difficulties in obtaining a highly periodic result in the experiments. One of the difficulties is related to the generation of the regular incident wave. For Case #004 and #014 the target wave high of the long-crested regular deep-water wave is 8 m. From the measurements, the average wave height for Case #004 is 8.3 m and 8.6 m for Case #014. If the responses are purely linear, the measurements can be adjusted linearly with the wave height. The actual responses, however, can be highly non-linear as will be shown with Case #014, making a simple linear scaling impossible.

4.1 Case #004

The experimental results and the numerical predictions of the heave and pitch motion for Case #004 are shown in Fig. 3. The predicted motions agree very well with the measurement. The ratio between the wave length and the ship length is approximately $\lambda / L_{pp} \approx 1$ yielding a large pitch motion. The start-up time for the CFD method (OpenFOAM) is relatively long requiring a huge processing time and power. The start-up time for the two-way coupling scheme is longer than the one-way coupling scheme because the two-way coupling scheme requires the initial deformation of the hull girder to be in equilibrium with the flow.

The vertical bending moment amidships is shown in Fig. 4. Differences between the magnitudes of the sagging and hogging VBMs are clearly seen in the measurement and in the CFD results. The sign convention applied in this paper is that hogging VBM is positive and sagging VBM is negative. In Fig. 4 it is observed that the wave induced sagging VBM is

approximately 40% larger than the hogging VBM. The peak-to-peak prediction from the non-linear strip theory (Shipstar) agrees with the measurements, but there is less difference between the sagging and hogging VBM in the Shipstar results. A standard linear strip theory calculation yields a VBM amplitude equal to 3900 MNm.

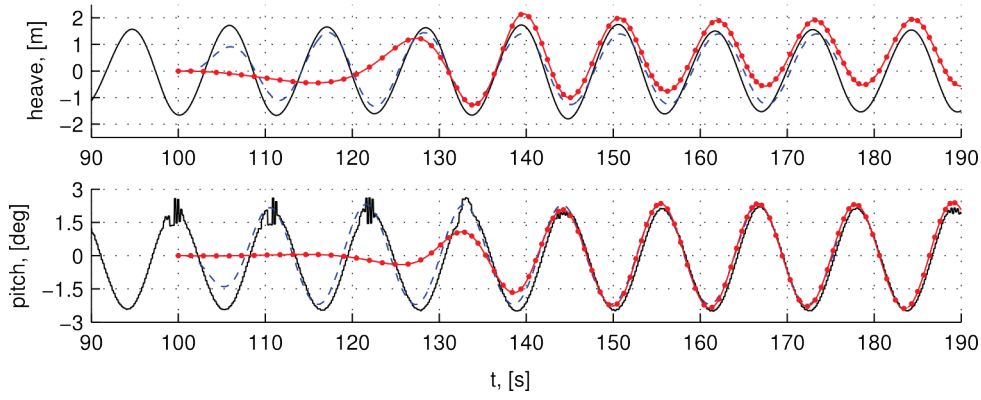

Figure 3: Heave and pitch motion, Case #004: Exp. CEHIPAR (——); OpenFOAM 2-way coupled (—●—); Shipstar flexible model (– – –)

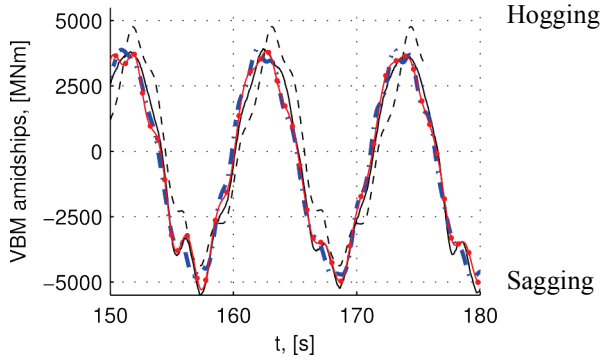

Figure 4: VBM amidships, Case #004: Exp. CEHIPAR (——); Shipstar flexible model (– – –); OpenFOAM 1-way coupled (– . –); OpenFOAM 2-way coupled (—●—)

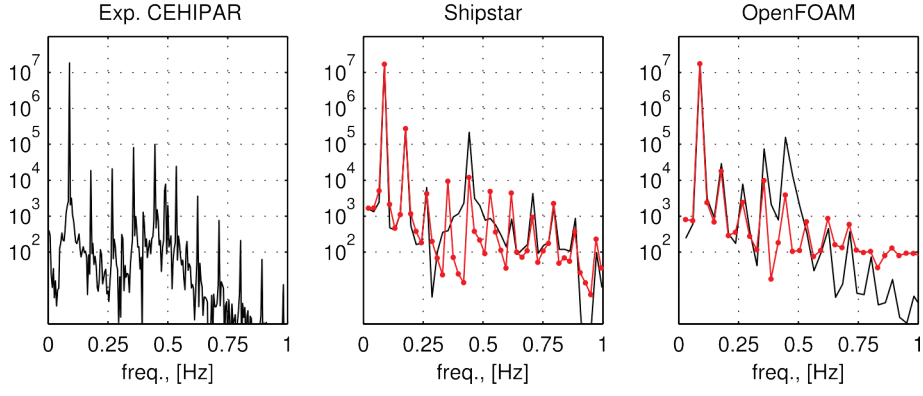

Figure 5: Power spectrum of amidships VBM, Case #004; Exp. CEHIPAR (Left); Shipstar flexible model (Middel,——); Shipstar rigid model (Middel,—●—); OpenFOAM flexible 2-way coupled (Right,——); OpenFOAM rigid model (Right,—●—)

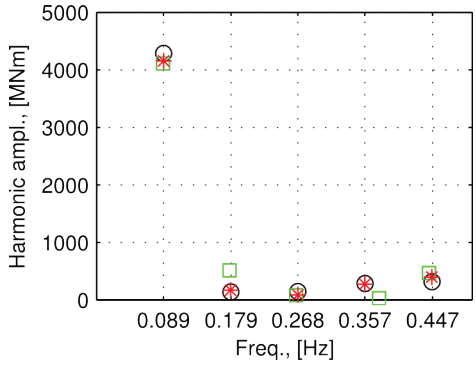

Figure 6: Amplitude of the lowest 5 harmonics, Case #004: Exp. CEHIPAR (○), Shipstar flexible model (□), OpenFOAM flexible 2-way coupled (✳)

Figure 4 shows that the results of using two-way coupling scheme (solid-dot line) agree almost perfectly with the measurements. The error in the peak values are less than 5 %. This error shall be interpreted with respect to the fact that the wave height generated in the experiment has a relative error of 4 %; see Table 2. A spectral analysis (FFT) of the responses shows that the response induced by the elastic vibration on the hull girder is one order of magnitude smaller than the responses of the rigid body motion (see Fig. 5 and 6) i.e. the hydroelastic effect is small and the application of the one-way coupling is feasible. As seen in Fig. 4 (dashed-dot line) the peak values of the VBM amidships predicted by the one-way coupling are still well within 5 % error. Overall, all calculations: linear and non-linear strip theory and CFD one- and two-ways are in good agreement with the measurements as regards the peak-to-peak value, but only the CFD calculations yields the same ratio between the hogging and sagging VBM as found in the measurements.

4.2 Case #014

The only change in the setup is the period of the regular incident wave. In Case #004, the target period is 14.9 s and in Case #014 it is 11.66 s. As presented in Table 2 the wave generated in the experiment has an average error of 8.25 % in wave height. For comparison purposes, the incident wave in the free surface CFD simulation is defined with the same mean wave properties as seen in the measurement. The predicted responses of the ship are shown in Fig. 7. Clearly, the peak values of the VBM amidships predicted by the CFD method and the non-linear strip theory are smaller than found in the measurement. The differences are about 35 %. Only the numerical results using the flexible beam model (CFD method or the strip theory) predict the same variation of the VBM amidships as seen in the measurement, cf. Fig. 7 and 8. However, whereas the phases and frequencies of the lower and higher harmonics agree, the amplitudes are smaller in the strip theory and CFD results. The linear strip theory predicts VBM amplitudes of about 3000 MNm and therefore provides nearly the same peak-to-peak values as found in the non-linear calculations, but does not follow the measured time domain variation.

The power spectrum of the responses of the rigid body simulation shows that the responses are non-linear. The 1st harmonic seen in Fig. 9 corresponds to the encounter frequency of the incident wave. Over-harmonic frequencies of 2nd, 3rd, 4th and 5th multiples of the encounter wave frequency can be clearly identified. A comparison between the power spectrum of rigid body responses and the responses predicted by the flexible beam model suggests that the 4th over-harmonic frequency coincides with the eigenfrequency of the wetted two-node vertical bending vibration causing a resonance. The same can be observed in the measurement except that the amplitude of the 4th harmonic is about 50% smaller in the numerical results cf. Fig. 10. Assuming that the responses are linear in wave height, the error in wave height seen in the experiments should account only for 8.25 %. However, the responses are non-linear and there is a

resonance. An amplification of the error from 8.25 % at the input to 35 % at the output (i.e. an amplification factor of 4) seems to be a possible scenario.

Between the non-linear strip theory and the free surface CFD, the results are very similar demonstrating the usefulness of the strip theory in a practical engineering application. It shall be emphasised, however, that no severe slamming is encountered in the present wave configuration. The type of hydroelastic responses seen here can therefore be classified as a springing vibration where over-harmonics in the incident wave and in the non-linear hydrodynamic responses induce a resonance excitation of the two-node vertical bending mode. With the significant vibration seen here it is clear that the classical one-way coupling approach is not feasible (see Fig. 8) as the hydroelastic effect of the hull girder vibration in resonance cannot be captured resulting in an amplitude of the two-node vertical bending vibration one order of magnitude smaller than in the two-way coupling approach. Using the results of the two-way coupling as the base for the evaluation of the hydroelastic effect, the prediction from the one-way coupling is off as much as 16% (peak-to-peak value). If the ship is considered rigid the error in the peak-to-peak value is approximately 22%. In both measurements and calculations the maximum sagging bending moment is slightly larger than the maximum hogging bending moment (Fig. 7). The issue here is that the local deformation of the hull girder is not transferred back to the fluid solver in the one-way coupling approach causing the added mass associated with the local vibrations to be completely missing in *f(x)*, see Eqs. (2). To improve the prediction of the one-way coupling scheme one may choose to model the missing added mass and include it explicitly in Eqs. (2b). Doing so, however, one will loose the benefit of having a high accuracy and implicitness in the CFD simulation.

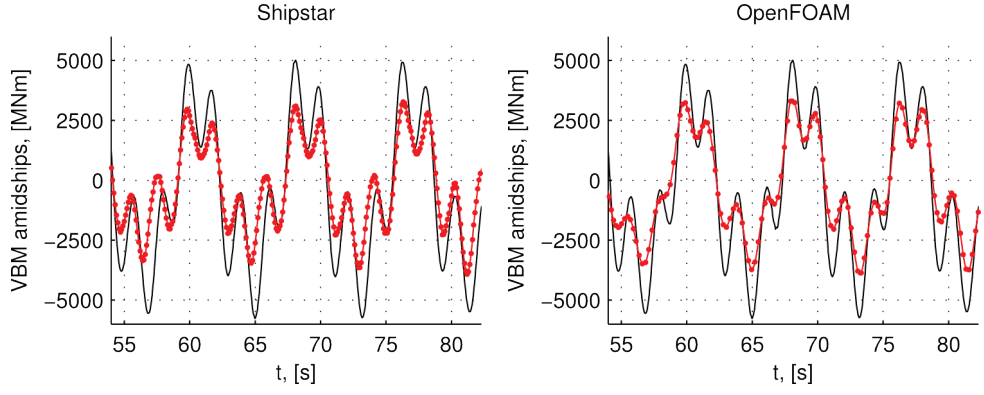

Figure 7: VBM amidships, Case #014: Exp. CEHIPAR (——); Shipstar flexible model (Left, —●—); OpenFOAM 2-way coupled (Right, —●—)

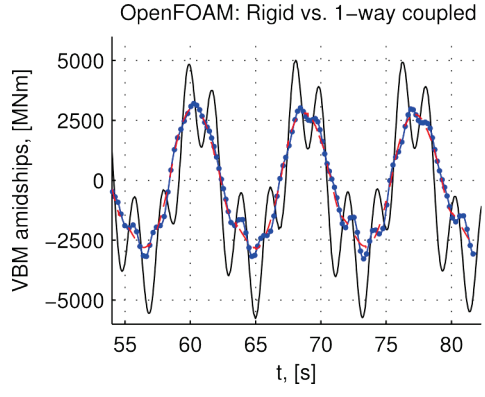

Figure 8: VBM amidships, Case #014, Exp. CEHIPAR (——); OpenFOAM rigid model (– – –); OpenFOAM 1-way coupled (—●—)

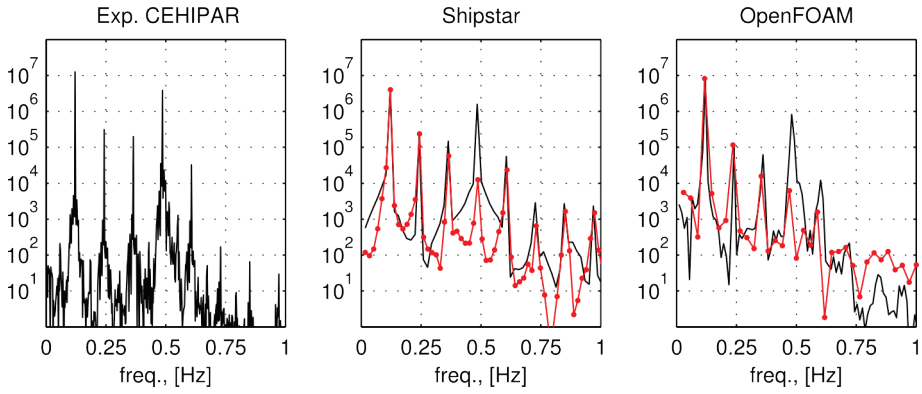

Figure 9: Power spectrum of amidships VBM, Case #014; Exp. CEHIPAR (Left); Shipstar flexible model (Middel, ——); Shipstar rigid model (Middel, —●—); OpenFOAM flexible 2-way coupled (Right, ——); OpenFOAM rigid model (Right, —●—)

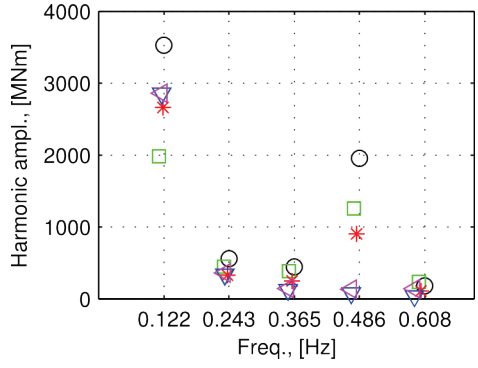

Figure 10: Amplitude of the lowest 5 harmonics, Case #014: Exp. CEHIPAR (○); Shipstar flexible model (□); OpenFOAM flexible 2-way coupled (✳); OpenFOAM rigid model (▽); OpenFOAM flexible 1-way coupled (◁)

5. CONCLUSION

Two methods, a free surface CFD and a non-linear strip theory have been applied to evaluate the hydroelastic effect in a post-Panamax ship sailing head sea. The results are compared with measurements for a flexible model of the vessel. A very good agreement between the numerical results and the measurements in regular long-crested wave, Case #004, with wave length close to the ship length is found. The non-linearity in the responses is almost negligible and both methods predict the frequency contents and the amplitude of each harmonic very well. The hydroelastic effect contributes about 7% to the overall peak-to-peak VBM. In another wave configuration, Case #014, the 4th harmonic of the non-linear hydrodynamic forces coincides with the two-node vertical bending vibration inducing springing resonance. The resonance behaviour is correctly predicted by both methods except that the amplitude of the 1st and the 4th harmonic are significantly smaller in the numerical predictions. Even though the wave height is a main source of error in the model tests no satisfactory explanation can be found on why the predicted amplitude of the 1st harmonic is 45% smaller than the measurements.

There is no indication of severe slamming in the two cases considered. The responses can therefore be categorized as a springing of the hull girder and the non-linear strip theory seems to be a very efficient tool for estimating the hydroelastic responses. As seen in the present evaluation the strip theory is nearly as accurate as the direct CFD calculation.

ACKNOWLEDGEMENT

The first author is grateful for financial support from American Bureau of Shipping (ABS) and from the Danish Maritime Fund. Part of the present work is financed by EU FP7 project TULCS (Tools for Ultra Large Container Ships), project no. 234146. The fruitful cooperation with the project partners, in particular Jos Konig from MARIN, Netherlands, Adolfo Maron from CEHIPAR, Spain and Sime Malenica from Bureau Veritas, France, is greatly appreciated.

REFERENCES

1. Aalberts, P. J. and Nieuwenhuijs, M. W., Full Scale Wave and Whipping Induced Hull Girder Loads. *Hydroelasticity in Marine Technology,* 2006, 65-78.
2. Zhu, S., Wu, M. and Moan, T., Experimental investigation of hull girder vibrations of a flexible backbone model in bending and torsion, *Applied Ocean Research,* 2011, 33, 252– 274.
3. Miyake, R., Matsumoto, T., Zhu, T., Usami, A. and Dobashi, H., Experimental studies on the hydroelastic responses using a flexible mega-container ship model, *Hydroelasticity in Marine Technology*, 2009, 161-171.
4. Bishop, R.E.D. and Price, W.G., *Hydroelasticity of Ships,* Cambridge University Press, 1979.
5. Xia, J.Z., Wang, Z.H., Jensen, J.J., 1998, Non-linear wave loads and ship responses by a time-domain strip theory, *Marine Structures*, 11 (3), 101–123.
6. Hirdaris, S. E., Miao, S. H. and Temarel, P., The effect of structural discontinuity on antisymmetric response of a container ship, *Hydroelasticity in Marine Technology*, 2009, 57-68.
7. Senjanović, I., Tomašević, S., Vladimir, N., Tomić, M. and Malenica, Š., Ship hydroelastic analysis with sophisticated beam model and consistent restoring stiffness, *Hydroelasticity in Marine Technology*, 2009, 69-80.
8. el Moctar, O., Oberhagemann, J. and Schellin, T.E., Free surface RANS method for hull girder springing and whipping, *SNAME Transaction*, 2011 (accepted for publication).
9. Tick, L., Differential Equations with Frequency-Dependent Coefficients, *Journal of Ship Research*, 1959, 3, 45–46.
10. Yeung, R. W., A Singularity Distribution Method for Free-Surface Flow Problems with an Oscillating Body, *University of California, College of Engineering*, 1973, Rep. No. NA 73-6.
11. Andersen, I.M.V. and Jensen, J. J., 2012. On the effect of hull girder flexibility on the vertical wave bending moment for ultra large container vessels. *OMAE*, 2012 (accepted for presentation).
12. Berberović, E., van Hinsberg, N. P., Jakirlić, S., Roisman, I. V., and Tropea, C., Drop impact onto a liquid layer of finite thickness: Dynamics of the cavity evolution, *Phys. Rev. E*, 2009, 79(3):036306.
13. Jasak, H., and Tuković, Z., Automatic mesh motion for the unstructured finite volume method. *Transactions of FAMENA,* 2007, ***v30***.
14. Seng, S., Jensen, J. J., and Pedersen, P. T., Numerical prediction of slamming loads, *Journal of Engineering for the Maritime Environment*, 2012.
15. Seng, S. and Jensen, J. J., Slamming simulations in a conditional wave. *OMAE*, 2012, 83310 (accepted for presentation).
16. Jensen, J. J., *Load and Global Response of Ships*, Elsevier, 2001.
17. Collatz, L., Eigenwertaufgaben mit technischen anwendungen, Akademische Verlagsgesellschaft, Leipzig, 1963.
18. Fenton, J. D., The numerical solution of steady water wave problems, *Computers & Geosciences,* 1988, Vol. 14, No. 3, 357-368.